Control of Thermal Distribution in Additive Manufacturing

by

Aniket Chandrashekhar Jadhav

A thesis submitted in partial fulfillment
of the requirements for the degree of
Master of Science in Engineering
(Automotive Systems Engineering)
in the University of Michigan-Dearborn
2018

Master's Thesis Committee:

Professor Pravansu S. Mohanty, Chair
Associate Professor Gargi Ghosh
Associate Professor Tanjore V. Jayaraman

Acknowledgements

I would like to thank my parents Mr. Chandrashekhar S Jadhav and Mrs. Uma C Jadhav for their unparalleled love and support. It is their blessings and belief that motivate me to through thick and thin. I also would like to thank my family for their constant support. I would like to express my gratitude to my Professor Dr. Pravansu Mohanty for this unique opportunity to work and learn at the Additive Manufacturing Processes Laboratory in the field of Powder Bed Fusion Processes. He has always been a strong inspiration and motivation for me and has led me by example that only hard work and efforts help you achieve greater things.

This study wouldn't be as constructive without the support of my teammates Ramcharan Palacode Visveswaran, Dr. Vikram Varadaraajan, Sharan Kumar Nagendiran, Zhuoran Wang, Neeraj Karmarkar, Sujeet Shinde and Anup Bapat. I would like to thank them for helping me in any and every way possible.

Table of Contents

List of Figures

List of Tables

Abstract

Additive Manufacturing is a rapidly growing industry. However, the defects generally occurring in parts built through Additive Manufacturing have hindered its way towards a reliable technology for mass production. Most of these defects generally occur through residual stresses building up in the parts during the process. Complex machinery is available which ensures defect free parts but it comes with a trade-off for cost.

The aim of this study is to provide a potential cost-effective solution to address the defects and issues arising due to uneven thermal distribution in the AM built parts. A detailed study about the basic understanding of the consolidation mechanism of the Powder Bed based Additive Manufacturing processes and Induction is discussed. The use of induction to selectively control the thermal distribution in these manufacturing process is proposed. Preliminary stage simulations and experiments are carried out to validate the proposal and its scope of application is discussed

Chapter 1 Introduction

1.A Additive Manufacturing

In contrast to Conventional Manufacturing, also known as Subtractive Manufacturing, Additive Manufacturing, a comparatively new process, completely eliminates machining operations such as milling, lathing, turning, wire EDM, carving, etc. [1]. This, not only, significantly reduces the production cost and time but also helps eliminating production material wastes as an outcome of the process. Additive Manufacturing, as defined by American Society for Testing and Materials (ASTM) is "a process of joining materials to make objects from 3D model data, usually layer upon layer, as opposed to subtractive manufacturing methodologies" [2]. The working principle of this manufacturing technique gives an advantage of iterating the process with a window for minor modifications to the object design to be built with minimal or no material losses. ASTM further categorizes Additive Manufacturing into seven categories. They are- Binder Jetting, Directed Energy Deposition, Material Extrusion, Material Jetting, Powder Bed Fusion, Sheet Lamination and vat photopolymerization [2]. Additive Manufacturing, also popularly known as 3D Printing, a term, synonymously used, relates to machines that are low-end in price and/or overall capability [2]. As per the Wohler's Report 2016, the 3D Printing Industry has surpassed $5.1 Billion and has seen a proverbial Hockey Stick (growth that moves rapidly from horizontal to vertical). With a Compound Annual Growth Rate of 25.9% from 2015

and a constant 26.2% for the past 27 years [3], this 31 year old manufacturing process traces its origin in 1986. Charles Hull developed and patented a technique called "stereo-lithography" which involved the use of lasers for burning and combining layers of resin to form a three dimensional object. In 1991, three AM technologies were commercialized, namely, the FDM (Fused Deposition Modelling), SCG (Solid Ground Curing) and LOM (Laminated Object Manufacturing) by Stratasys, Cubital and Helisys respectively [10]. However, it was only in 1993, the Massachusetts Institute of Technology introduced Three Dimensional Printing (3DP) [4]. Selective Laser Sintering was developed and created by Carl Deckard at the University of Texas at Austin in 1980[11]. The years 1999 to 2002 witnessed rapid growth of Additive Manufacturing in the medical field. Engineered organs and implants were 3D printed and coated with the patient's own cells with a minimal or no risk of rejection by the immune system. Mini functional kidney capable of filtering blood and diluting urine was developed using the 3D Printing technology. The first SLS (Selective Laser Sintering) machine was developed in 2006 whereas the Urbee, the world's first 3D printed environment-friendly car was manufactured in 2011 following the first 3D Printed Aircraft completed in a mere 7 day period for a budget of £5000 in 2010 [12].

1.B Additive Manufacturing and Mass Customization

Additive Manufacturing has been compared as well as been contrasted with mass customization. While 3D printing uses CAD Software and Additive Manufacturing technologies to fuse a variety of materials, mass-customization relies on either using various combinations of pre-assembled modular parts or components. The raw materials

typically used up in mass customization are component parts whereas 3D Printing makes use of raw material such as plastics, super alloys, resins, metals, in the form of powders, wires, etc. The following table gives a descriptive comparison between Additive Manufacturing and Mass customization based on different characteristics [13].

Characteristic	Mass Customization	3-D Printing
Manufacturing Technology	Based on pre-assembled modular parts in different combinations or delayed differentiation.	Automated manufacturing based on CAD software and additive manufacturing.
Supply Chain Integration Requirements	Need for highly-integrated supply-chain management to ensure right goods at right times from multiple supplies.	Uses readily available supplies available from multiple vendors.
Economic Benefits	Ability to produce custom products at relatively low prices. Low inventory risk. Improved working capital management.	Ability to produce custom products at relatively low prices. Low inventory risk. Improved working capital management.
Range of Products	Computers; watches; windows; shoes; jeans.	Prototypes; mockups; replacement parts; dental crowns; artificial limbs.

Table 1.1: Comparison between Mass Customization and Additive Manufacturing [13]

1.C Powder Bed Fusion Processes

As mentioned earlier, Additive Manufacturing is categorized in seven families. The entire scope of this thesis is emphasized on one of these families, namely, Powder Bed Fusion process. It is a process in which the powdered materials are consolidated together by melting them using a heat source like a Laser or an Electron beam. The powder surrounding the workpiece acts as support for overhanging structures, etc [5]. The powder bed fusion process is further classified into different processes i.e., Direct Metal Laser Sintering (DMLS), Electron Beam Melting (EBM), Selective Laser Sintering (SLS) and Selective Heat Sintering (SHS). A typical pictorial representation of the powder bed fusion process is as shown in the following figure.

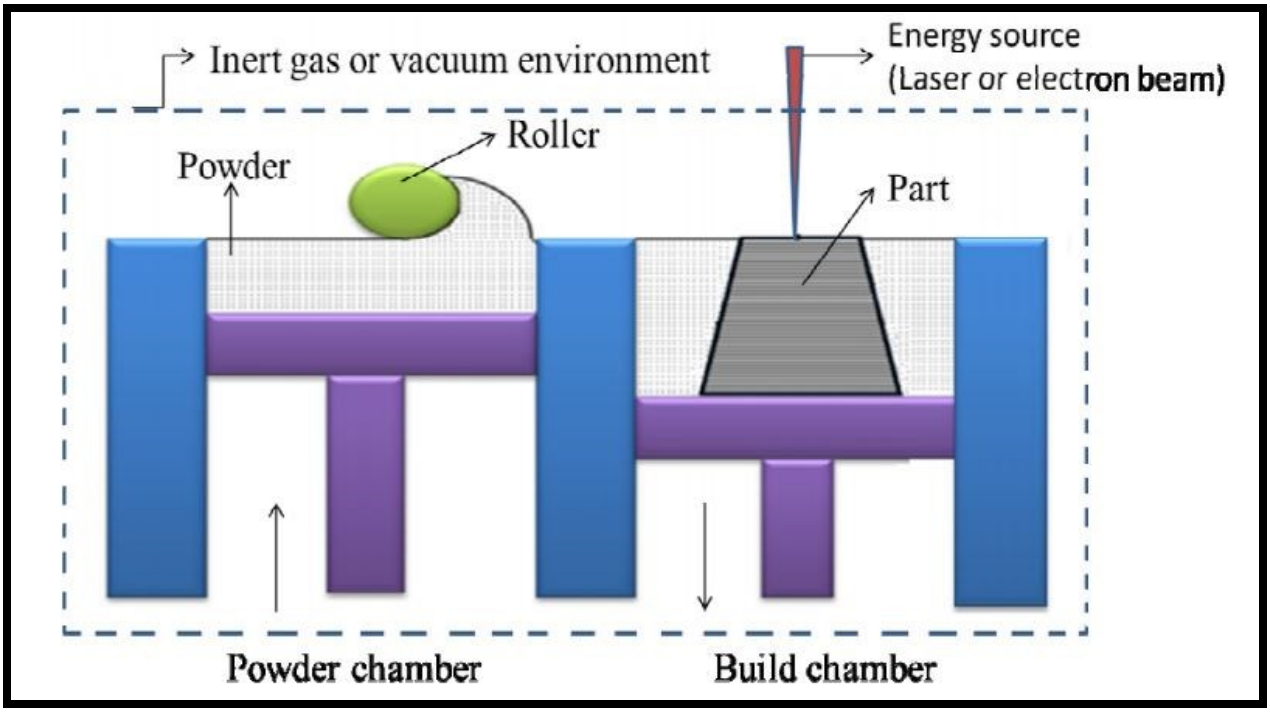

Figure 1.1: Powder Bed Fusion Process [21]

Chapter 2 Powder Bed Fusion Process

2.A. Overview

Powder Bed Fusion is a process used to produce objects from powdered materials using one or more lasers to selectively fuse or melt the particles at the surface, layer by layer, in an enclosed chamber [2]. Consolidation in in this process mainly can be induced in five different ways: solid state sintering, liquid state sintering, chemical induced binding, partial melting and full melting. However, due to the slow scan speed requirements of solid state sintering to maintain high temperatures for sufficient time to allow diffusion of atoms, this technique proves inefficient with respect to economic manufacturing. Given these limitations, Powder Bed Fusion still allows high complexity components to be manufactured with the powder material acting as support structures throughout the process. Consolidation by partial melting (usually referred to as Selective Laser Sintering) and full melting (usually referred to as Selective Laser Melting) are mostly (±95%) used for processing Polyamide-12; a typical nylon grade. SLS and SLM for metal use is still limited to Stainless Steel and a few grades of Tool Steel whereas Titanium (Ti6Al4V) and Aluminum have started finding industrial applications [6]. Laser Sintering is a short-time interval process (in the order of milliseconds). As a result of this, binding through partial melting of the powder becomes a practical approach. This is done usually by applying a laser source to locally melt the lower melting point powder of the combination of the

powder to be sintered. This, then wets the higher melting point powder and binds it together to form a sintered layer. Inter-particle wetting done by this two-phase approach is important to avoid the "balling phenomena" [14]. Due to the partial melting of the powder, a more liquid phase is present along the surface and the grain boundaries of the powder. This gives rise to a sintering-pool consisting a liquid-solid mixture. The high intensity Laser with a faster scan speed causes rapid solidification of the sintering pool. As metal SLS demands higher temperatures for the binding mechanism to take place, severe oxidation might be involved. Oxidation of such laser processed metals leads to the formation of metal-ceramic interfaces in the sintering pool lowering the liquid-solid wettability and causing balling. Therefore, the balling phenomena occurs when the laser melted powder does not wet the remaining solid powder and the underlying substrate layer due to the contaminated layer of metal oxide present in the pool [15].

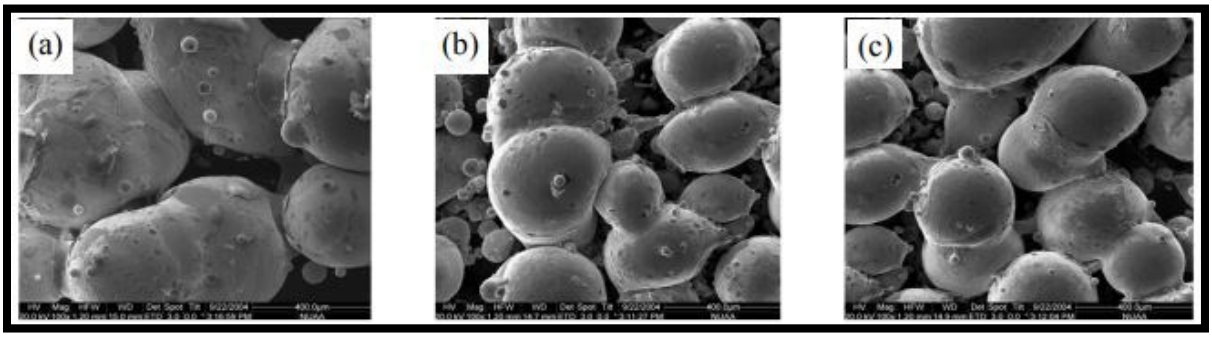

Figure 2.1: SEM images of balls formed at a fixed laser power of 300W but different scan speeds of (a) 0.05m/s, (b) 0.08m/s, and (c) 0.1m/s [1]

2.B. Materials

A wide range of materials have been tested out and are also currently used in the SLS process. The materials include wax, cermet, ceramics, nylon/glass composite, metal-polymer powders, metals, alloys or steels, polymers, nylon and carbonates. A number of metal systems (e.g., Fe-Cu, Fe-Sn, Cu-Sn), metals (e.g., Al, Cr,4 Ti,42 Fe, Cu), ceramics (Al2 O3 , FeO, NiO, ZrO2 , SiO2 , CuO) and alloys (e.g., cobalt-based, nickel based, bronze-nickel, pre-alloyed bronze-nickel, Inconel 625, Ti6Al-4V, stainless steel, gas-atomized stainless steel 316L, AISI 1018 carbon steel, high-speed steel, pre-coated foundry sand and alumina with polymer binder) are also being tested for SLS [14].

2.C. Experimental Parameters

The powder density, size, shape and its distribution monitors the sintering process of the powders. To improve sintering, the density of the metal needs to be improved. This can be achieved by optimizing the particle shape and surface state of the powder. As a result of this, prior to the SLS process, the sinterability of the powder needs to be improved. This can be achieved through the electrostatic technique or through thermal treatment of the powders.

In addition to this, the scan speed, laser power, laser beam size, layer thickness, scan-spacing, powder bed temperature, etc. are the parameters that also need to be taken into consideration. Orientation of workpiece and packing of geometry also needs to be optimized in order to make maximum utilization of the build area and the pre-processed powders. The effects of these parameter can, however, not be generalized. A high energy

density laser beam helps in polymer sintering but a laser density greater than a critical value results in polymer degradation. A higher laser power for high-speed-steel-powders induces high surface density but at the same time it also increases surface roughness and inaccuracy of the part size. Any deviation from the optimal values of these experimental parameters, thus, leads to defects in the built parts. However, to overcome this, SLS parts can be post-processed. This improves the structural integrity, mechanical properties, surface roughness and most importantly, it decreases the porosity of the parts. One way of achieving this is through thermal treatment of the sintered parts. Selective LASER Sintering / Hot Isostatic Pressing (HIP) is a net-shaped manufacturing technique developed to fabricate high-density SLS parts. The HIP is a technique used to create an inert atmosphere at a specific pressure and temperature condition using inert gases. This helps in reducing the risk of oxidation and porosity in the SLS parts as the inert gas does not allow the material to chemically react [14].

Chapter 3 Thermal Distribution in Powder Bed

3.A. Consolidation mechanism in SLS and SLM

Liquid Phase Sintering and partial melting are the consolidation mechanisms that are followed in SLS, as discussed briefly in the previous chapter. This binding mechanism includes partially melting the powder material while the other part remains solid. The capillary forces arising due to the partial liquefaction of the powder material force the powder to spread itself instantaneously in the still solid powder particles. Due to this, higher scan velocities become possible. The material that melts maybe different than the one that remains solid. The former "lower melting point" material is then called the binder and the "higher melting point" material is called the structural material. Different ways to bind these two materials exist. They are as follows:

- Mixture of two-component powder (separate binder and structural powder particles).
- Using a composite powder that has a micro-composite structure containing the structural and binder material.
- Using coated particles in which the binding material is applied as a coating on the structural material. The binder material absorbs all the incident laser radiation. This induces the intended melting of the binder.

In all of the above methods, the binding material may be permanent with the part or may be removed later through de-binding cycles. In either of the situations, a post-sintering process (thermal heat treatment or HIP) for densification of parts maybe necessary. Partial melting of powder materials is also achievable in cases where there is only a single phase powder i.e., no distinct binder or structural material. In such cases, the SLS experimental parameters are optimized in a way to partially melt the powder. The heat source (laser) in such a situation only provides heat to sufficiently melt the shell of the particle while the core of the particle remains solid. As a result of this, neck formation between different grains of the particles tale place which binds the powder particles together.

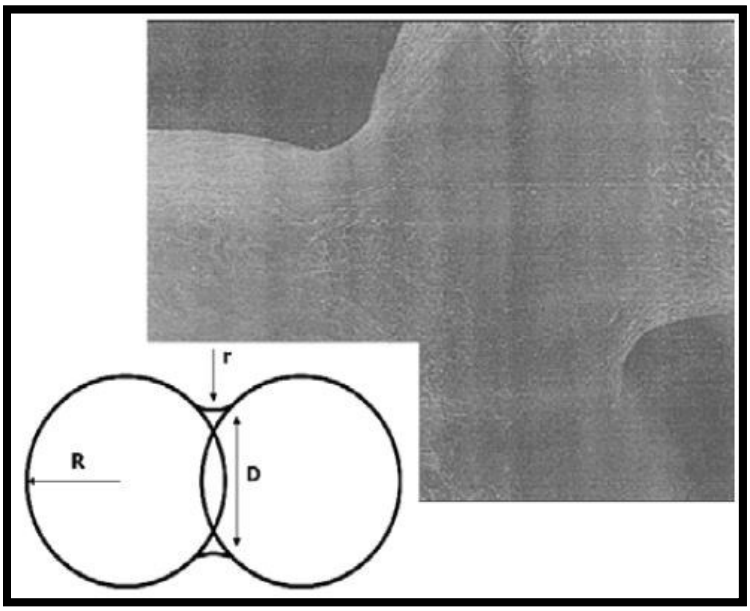

Figure 3.1: Typical neck formation between two stainless steel powder grains obtained through Nd:YAG Laser [16]

Partial melting can also be achieved with powders having a bi-modal distribution i.e., small particles are melted while the bigger particles remain solid. Partial melting proves more beneficial as compared to Complete or the Full Melting mechanism. It is because

drastically higher laser scan speeds and scan spacing become possible during partial melting of the powder particles even when aiming for full dense parts. The economic advantage thus possible is considerable against the need for post-densification of sintered parts.

One of the challenges faced during the consolidation is the controlling the flow of the heat source. The molten pool formed due to partial melting needs to wet the previously deposited layer as well for it to solidify and form a uniform layer. Also, during this, it must also form a flat upper surface for the next layer of powder to be spread and sintered. Since partial melting of the powder takes place at higher scan speeds, the only conditions acting upon the powder to be sintered are the thermal distribution, capillary and gravitational forces. This leads to porosity in the parts. Therefore, in order to achieve sufficient wetting of the previously deposited layer, excess energy needs to be supplied. This excess energy and the peak temperature has its effects on the topmost surface of the sintered part. Thermal gradients are formed in the melt pool. Due to this, there is a potential to form convective motions to reduce these gradients. Temperature gradients at the surface along with temperature dependent surface tensions can cause rapid motions known as the thermos-capillary flow or the Marangoni flow. The dimensionless Marangoni number (M_a) is given by equation (1):

$$M_a = \left(\left[\frac{d\gamma}{dx}\right]\left[\frac{w}{\eta}\right]\right) \Big/ \left(\frac{\kappa}{w}\right) \equiv \left(\left[\frac{d\gamma}{dT}\right]\left[\frac{dT}{dx}\right]\left[\frac{w}{\eta}\right]\right) \Big/ \left(\frac{\kappa}{w}\right) \quad \text{.....(1)}$$

It is defined as the ratio of the speed by which the surface temperature gradient (dT/dx) changes due to convection or conduction (w is the linear size of the pool and K is the thermal diffusivity). In case of Selective Laser Melting (SLM), there is a leading edge to the melting pool. This leading edge under the influence of the surface tension advances into the powder in the area around the Heat Affected Zone (HAZ). This advancement gives rise to a possibility of the powder around the HAZ, which is already at a temperature just below the solidus temperature, to be wetted by the melt pool's leading edge. The wetting or not of this solid powder and if it is wetted, its dragging into the molten pool adds further complications in the consolidation process. As a result of this, a compromise is always needed to balance either the good wetting or re-melting of the previously deposited layer along with the top most layer solidifying sufficiently flat and the powder bed not being disturbed too much ahead or around the dynamic HAZ. This adds a large constraint on metals and powder preparations for parts being fabricated through SLM.

In conclusion to the discussion of the consolidation phenomena and the effects of the process parameters on the same, a higher laser absorption in the powder bed reduces the variation in absorption throughout the powder bed. Smaller layer thickness with finer sized powder particles eases out the need to over-heat the layers if re-melting of the previous layers is necessary. This becomes possible due to its large surface-to-volume ratio. However, all of the above leads to the inability of consolidation at faster processing speeds [16].

3.B. Thermal Fluctuations and its effects

The basic mechanism of consolidation in any Additive Manufacturing process lies in the rapid heating and rapid solidification of the material being deposited, melted or sintered. The heat source providing the necessary temperature rise is Laser for SLS and SLM. During this process of rapid heating and solidification, the material to be sintered/melted undergoes many thermal excursions. As a result of this, residual stresses are induced in the part that is being built. The steep temperature gradient across the powder bed leads to different thermal expansions throughout the depth of the heating. The laser beam that is incident on the powder and the previously deposited layer coincides with the upper surface of the layer without initially melting the powder and the previous layer. This causes thermal stresses to be induced which causes bending of the upper layer of the part due to continuous heating. Initially, the layer under direct interaction of the laser bends in a direction away from the laser. This is known as counter bending. However, with continuous heating, the bending moment opposes the laser heat and starts bending towards the laser source and the mechanical properties of the material are reduced. During cooling, once the laser source is removed, the yield stress and Young's Modulus return back but to much higher levels inducing plastic re-straining. This phenomena through which thermal stresses are induced is known as the Thermal Gradient Mechanism [17, 18].

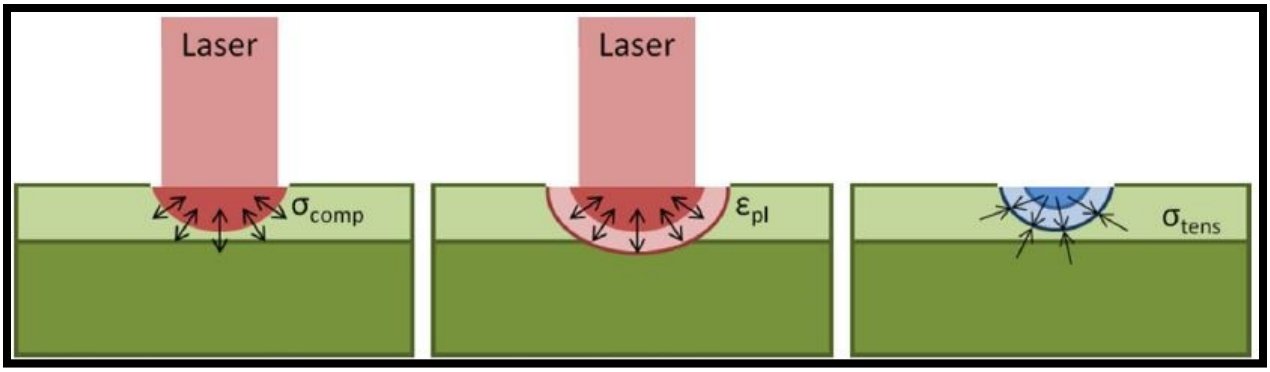

Figure 3.2: Stages of Thermal Gradient mechanism where σcomp, σtens and Ɛpl are the compressive stresses, tensile stresses and plastic strain respectively [18].

The changes in the build temperature and the physical changes occurring in the powder material leads to a distortion known as shrinkage. Shrinkage is a defect generated when the built part or the built layer of the part is actually smaller than the desired part or the layer. It mainly occurs due to an increase in the density of the built part or layer after solidification. The deviation in temperature in the build chamber also leads to different shrinkage rates with respect to the different build positions in the build chamber. The effect of the temperature of the working environment on the shrinkage ratio, is however, complicated and is non-linear in nature. The rate also gets affected by any changes in the activation energy. Curling of layers in SLS parts is another result of temperature deviation. This defect mainly occurs as a continuation of shrinkage. The different shrinkage rates, on the upper and lower sides of the layer which is sintered, between the areas which are sintered and those which are non-sintered develop curls [18].

3.C. Grain growth in powder metals

Ti6Al4V is the most widely used titanium alloy consisting of 6wt% Aluminum and 4wt% Vanadium. The high strength to density ratio, excellent material properties at elevated temperatures (up to 600 deg.C) with low density and excellent corrosion resistance makes it one of the most favorable metal alloys in Additive Manufacturing applications. Different microstructures of this alloy at various intermediate temperatures become possible by slow cooling during the laser deposition process of the alloy. The thermal cycle plays an important role into either forming martensitic structure or widmanstatten basketweave structure. Studies have shown that during the AM process of Ti6Al4V, the heat generated on the top of every layer determines the grain growth of single grain structures. The changes in the size, shape and crystal structure of the grains during the fabrication process determines properties of the alloy.

The columnar grain growth is a result of directional cooling and the thermal history of the material. An increase in the laser power decreases the length of these columnar grains which eventually are replaced by large equiaxed grains. This is also evident from the fact that there is a decrease in the temperature gradient from the first layer throughout the height of the built part. This occurs due to the higher laser power causing very high temperatures at the surface of the top layer and then remains to be hot during the sintering of the consequent layers.

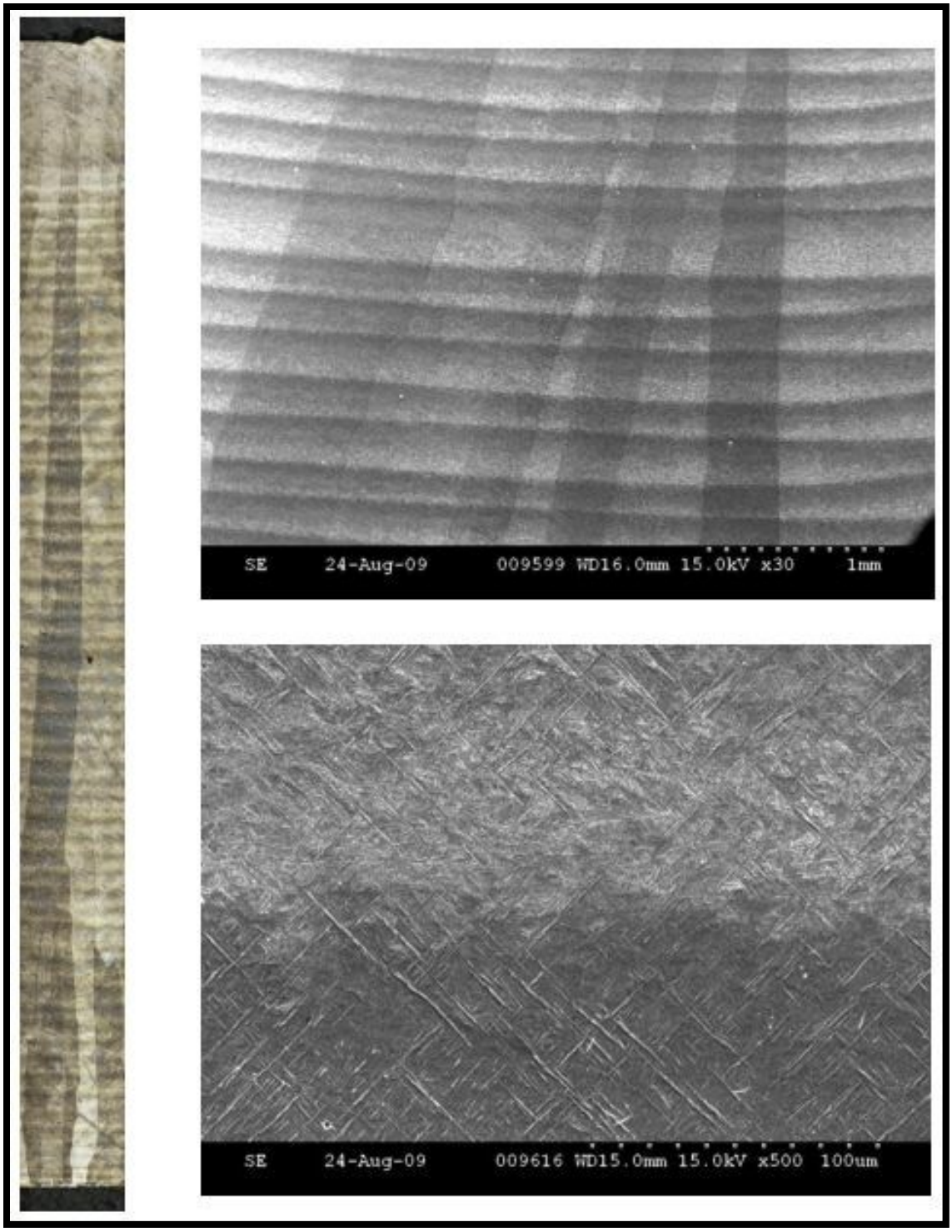

Figure 3.3: (a)Optical micrograph of the entire deposit showing the columnar grain growth (left), (b) SEM image at 30X of columnar grains throughout entire deposited length and width.(top right) and (c) SEM image showing the widmanstatten structure [26]

As can be seen from Fig.3.3, a columnar grain growth is obtained from the depositions as a part of the study. This grain growth, is a result of conduction of heat through the walls of the part built and also the build temperature which is maintained constant throughout the process. The microstructure layer obtained between the band layers is the basketweave widmanstatten structure. The widmanstatten structure is known to enhance material properties such as fracture toughness, creep notched fatigue resistance and fatigue crack growth resistance [26].

In order to enhance such material properties by maintaining constant thermal cycles and also to avoid or minimize any defects discussed in the sections above, thermal distribution with a controlled temperature gradient becomes important. Studies suggest that the temperature of the building chamber must be maintained just below the melting point of the materials in order to ensure desired quality of fabricated parts [19]. Trials have also been carried out to preheat the surface powders to ~0.5Tm to 0.6Tm, where Tm is the melting point, with the help of secondary lasers while the primary laser sinters the powder as per the chosen CAD geometry, in order to address shrinkage and curl development in ceramics [18]. The following figure illustrates the use of secondary laser to preheat the powder bed.

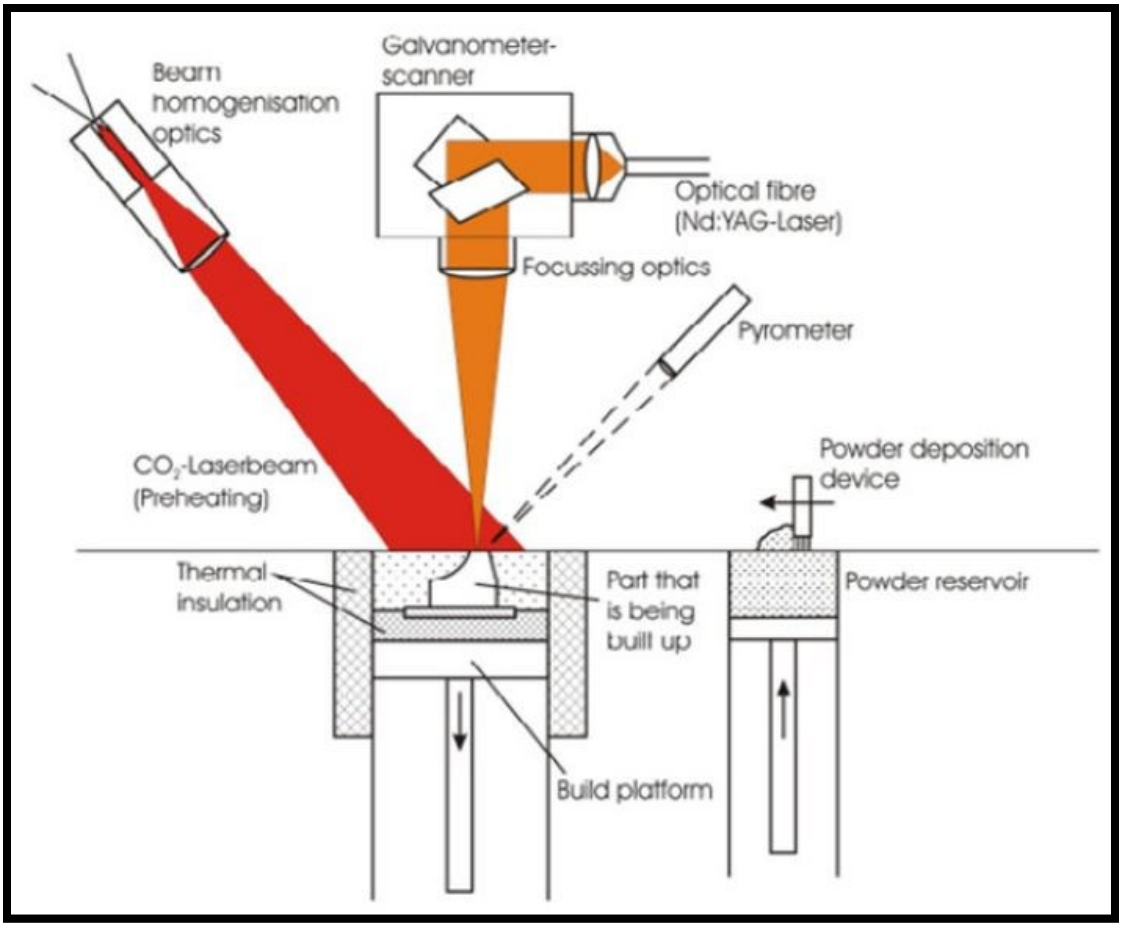

Figure 3.4: Pre-heating mechanism by CO2 laser [18]

However, making use of a secondary laser adds to the complexity of the entire process and asks for further optimization of process parameters. The goal is to not only address the issue of thermal fluctuation and steep thermal gradients in the powder bed but also to come up with solutions that lie well within the scope of modification or addition to the SLS/SLM process. The following chapter discusses Induction as a potential solution to address all the concerns mentioned in this chapter.

Chapter 4 Induction

Electromagnetic induction (or sometimes just induction) is a process where a conductor placed in a changing magnetic field (or a conductor moving through a stationary magnetic field) causes the production of a voltage across the conductor. This process of electromagnetic induction, in turn, causes an electrical current [7]. The process of electromagnetic induction is unique in its own way as it actually generates heat inside a component and/or a material that needs to be heated with no effect of inertia, high-power densities and adjustable penetration depths. The working principle for Induction is a combination of two laws in physics namely: Lenz's Law and Joule's Law. When any conductive substance is immersed in a varying magnetic field generated by an induction coil, the substance carries the induced electrical current, also known as Foucault Currents. According to the Joule effect, the movement of the electrons carrying these currents dissipates the heat in the substance where they are generated [8]. The quality of the energy inducted into the workpiece heavily depends on the placement of the inductor w.r.t. the part and vice versa, the frequency, magnetic, thermal and electric properties of the part to be heated, etc. The following factors have a pronounced effect on the way the induction system works:-

4.A. Electromagnetic Properties of the material

Electromagnetic properties of a material is a broader expression of numerous properties that define the electromagnetic characteristics of the material. A couple of the properties which have a significant effect on induction are discussed below:

1. **Electrical Resistivity -** The ability of a material to conduct electricity is known as the electrical conductivity of the material, σ. The reciprocal of this conductivity is known as electrical resistivity, ρ. The resistivity of a particular metal varies with temperature, chemical composition, metal microstructure and grain size. Metals having low electrical resistivities are known as good electrical conductors. However, metals are further classified based on their resistivities as low-resistive metals (silver, copper, gold, aluminum etc.) and high resistive metals (stainless steel, titanium, carbon steel, etc.). The resistivity for pure metals is often expressed as a linear function of temperature given by the equation:

$$\rho(T) = \rho 0\,[+\alpha(T - T0)]$$

Where $\rho 0$ is the resistivity at ambient temperature T0; ρ (T) is the resistivity at temperature T; α is the temperature co-efficient of electrical resistivity. The following graphs show electrical resistivities of some commercially used metals and their variation with temperature [9].

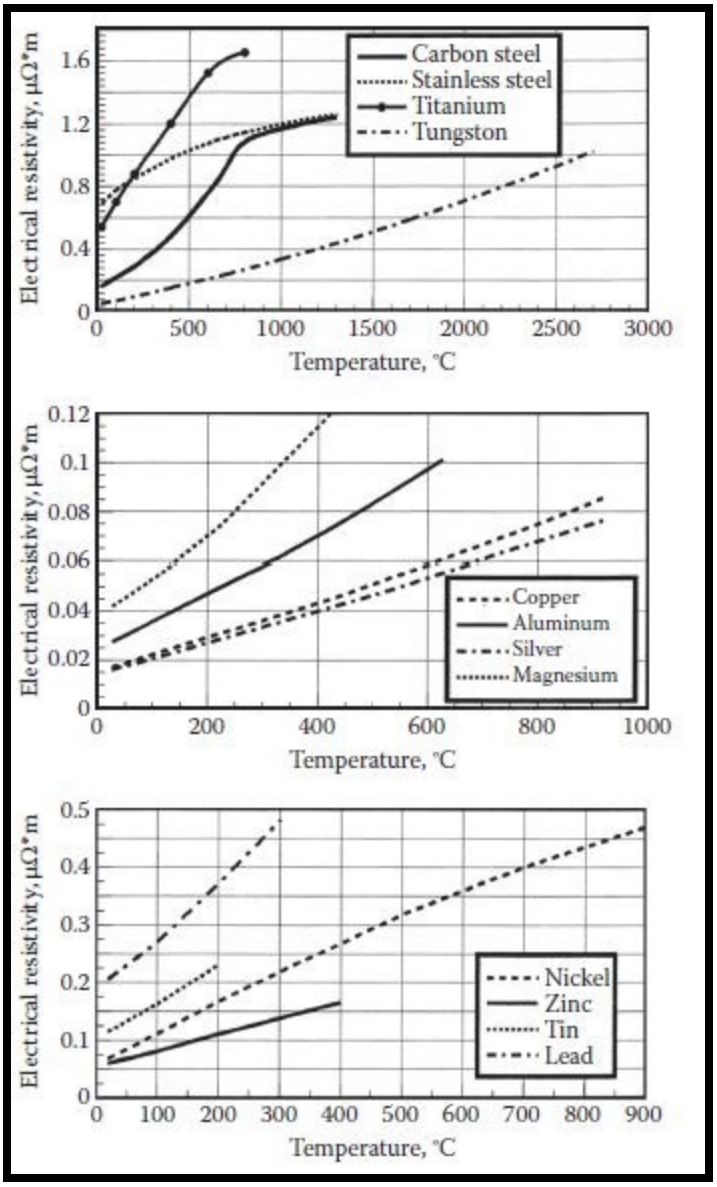

Figure 4.1: Electrical Resistivities of some commercially used metals [9]

2. **Magnetic Permeability and Relative Permittivity (Dielectric Constant) -** Relative magnetic permeability, μ_r, of a material is defined as the ability of the material to conduct magnetic flux better than a vacuum or air. Relative permittivity, ε, indicates the ability of a material to conduct electric field better than a vacuum or air. Both these properties are non-dimensional parameters, however, understanding

the physics of these properties is very important while designing induction heating systems. Relative magnetic permeability has a significant effect on all basic induction phenomena including the skin effect, electromagnetic edge and end effect, proximity and ring effects, coil calculations and computation of the electromagnetic field distributions. The constant $\mu_{0=4\pi}$ x 10^{-7} H/m [or Wb/ (A.m)] is known as the permeability of free space. The product of relative permeability and permeability of the free space is called permeability and is the ratio of magnetic flux density (B) to magnetic field intensity (H).

$$B / H = \mu_r\mu_0 \text{ or } B = \mu_r\mu_0 H$$

Based on the magnetization abilities, all materials are classified as paramagnetic, diamagnetic and ferromagnetic materials. Relative magnetic permeability of paramagnetic materials is slightly greater than unity. For diamagnetic materials, it is slightly less than 1. However, ferromagnetic materials exhibit very high values of relative permeability ($\mu r >> 1$). Ferromagnetic properties of a material heavily depend and are a complex function of structure, chemical composition, prior treatment, grain size, frequency, magnetic field and temperature. For example, a same kind of carbon steel at same temperature and frequency will have different values of relative magnetic permeability due to differences in the magnetic field intensity [9].

4.B. Skin Effect

The current distribution in a conductor carrying direct current is always uniform throughout its cross-section. However, when an alternating current is passed through the same conductor, there is uneven distribution of electric current. The maximum value of current density will always be found at the surface of the conductor. This density goes on decreasing from the surface towards the core of the conductor. This phenomenon of non-uniform distribution of current within the conductor's cross-section is known as skin-effect. As a result of this, skin effect is also found in the workpiece meant to be heated/ treated through induction, due to the presence of an alternating current. This is one of the major reasons behind the concentration of eddy currents on the surface (skin) layer of the workpiece. In electrical applications, approximately 86% of the power is found to be concentrated in the surface layer of the conductor. This layer is known as the reference (or penetration) depth, δ. The extent of skin effect depends on the frequency of the system and also the material properties of the conductor.

$$\delta = 503\sqrt{\frac{\rho}{\mu r.F}}$$

Where δ is the penetration depth in meters, ρ is the electrical resistivity of the metal (Ω*m), μ_r is the relative magnetic permeability and F is the frequency in Hz [9].

4.C. Electromagnetic Proximity Effect

In most applications and systems, a current carrying conductor never stands alone. It is usually surrounded by other current carrying conductors or conductive materials. In such cases, the current and power density distribution gets distorted and is never uniform. This effect of the proximity of two current carrying conductors on their respective electromagnetic fields is known as the electromagnetic proximity effect.

Figure 4.2.a shows a representation of the skin effect in a conductor standing isolated. However, when another current carrying conductor is placed close to this conductor, the currents in both these conductors redistribute. If the currents flowing in both these conductors have opposite directions, then due to the skin effect, both currents will be concentrated in areas facing each other, as shown in Figure 4.2.b. This results in a strong magnetic field in the area between the two conductors. This results because of both the conductors having their respective magnetic field lines in the same direction. Due to a strong internal magnetic field, both these conductors will have a weak external magnetic field. On the other hand, if the currents flowing in the conductors have the same direction, the both the currents will be concentrated in areas opposite to each other, as shown in Figure 4.2.c. This would result in a weak magnetic field in the area between the two conductors. However, due to a weak internal field, both these conductors will have a very strong external magnetic field.

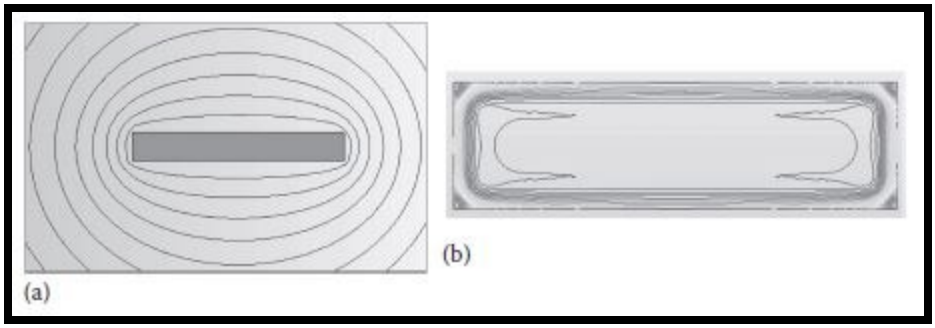

Figure 4.2.a:- (a) Magnetic field & (b) Current density distribution in a stand-alone conductor [9]

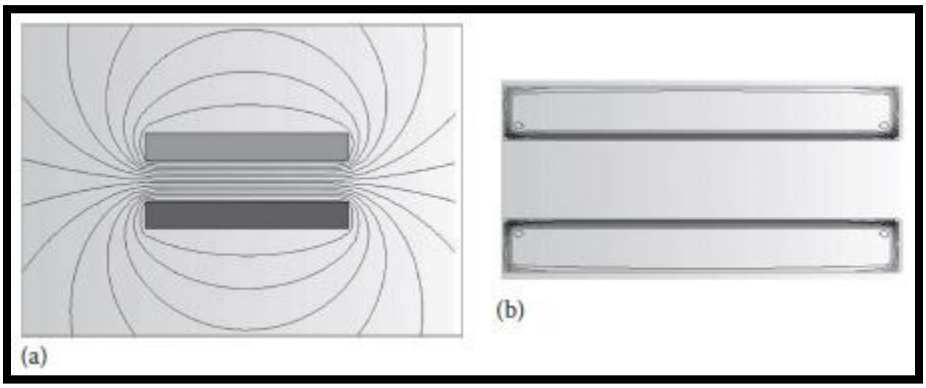

Figure 4.2.b:- (a) Magnetic field and (b) Current density distribution in conductors with current in same directions [9]

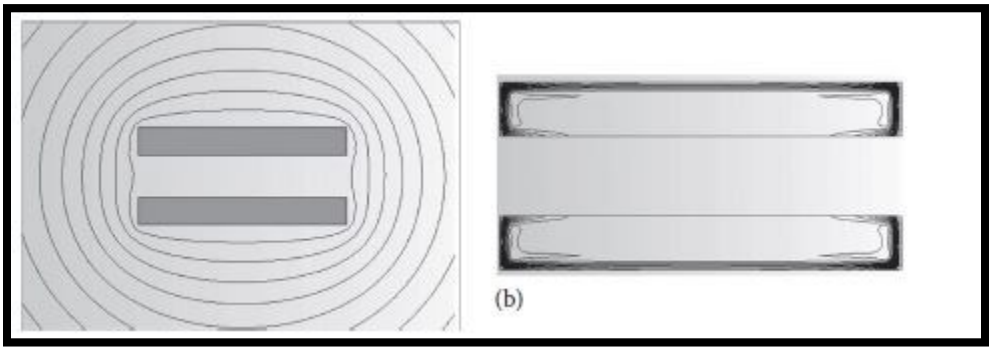

Figure 4.2.c:- (a) Magnetic field and (b) Current density distribution in conductors with current in opposite directions [9]

The phenomenon of proximity effect finds a direct application in Induction Heating. Here, the first conductor is the inductor carrying the current and the second conductor is the workpiece. According to Faraday's law, the direction of the eddy currents induced in the

workpiece would be in the opposite direction as that of the inductor. This, as per the proximity effect, would lead to a strong magnetic field between the inductor and the workpiece due to the eddy currents concentrating in the areas of the conductors that face each other [9].

4.D. Basic Thermal Phenomena in Induction Heating

The thermal properties of the materials play an important role in deciding the system requirements and parameters for induction heating. The Thermal Conductivity k defines the rate at which heat travels across a thermally conductive workpiece. In order to obtain a uniform thermal distribution, a metal with a higher thermal conductivity is preferred. However, in cases of selective heating, metals with higher k values may become a disadvantage. Metals with higher thermal conductivities have a tendency to promote soaking action and equalize thermal distribution within the workpiece. As a result of this, temperature rise not only takes place in the region of interest but also in areas surrounding it. Due to this, higher power is required to attain the desired temperature rise in the region of interest. Moreover, higher temperatures always bring in the possibility of geometric distortions in the workpiece.

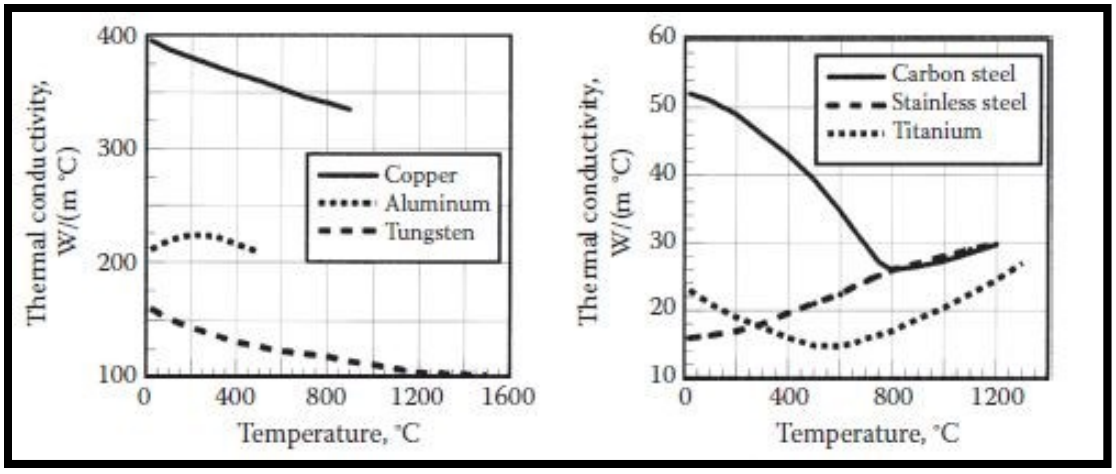

Figure 4.3: Thermal conductivities of metals Vs Temperature [9]

Similarly, the value of heat capacity C indicates the amount of energy that the workpiece would absorb in order to achieve a unit rise on temperature. Mathematically,

$C = dQ/dT$

Where dQ is the required energy and dT is the required temperature change. Heat capacity is closely related to a parameter called specific heat c which represents the heat capacity per unit mass i.e., the amount of energy absorbed by a unit mass of the workpiece to achieve a unit temperature increase [9].

4.D.1 Modes of Heat Transfer

Induction heating is characterized by three modes of heat transfer namely conduction, convection and radiation. Each mode of heat transfer plays a significant role depending on the nature of their application. They are discussed briefly as follows:-

4.D.1.1 Thermal Conduction

Heat Transfer through this mode takes place by conduction of heat from higher-temperature regions to lower-temperature regions as per Fourier's law,

$$q_{cond} = -k \, \text{grad}(T)$$

where q_{cond} is the heat flux by conduction and k is the thermal conductivity. As seen from the above equation, the rate of heat transfer through conduction is directly proportional to the temperature gradient and thermal conductivity of the material or the workpiece [9].

4.D.1.2 Thermal Convection

Heat transfer through convection is governed by Newton's law which states that the heat transfer rate through convection is directly proportional to the temperature difference between the workpiece surface and the ambient area. It is expressed as follows:

$$q_{conv} = \alpha (T_s - T_a)$$

where q_{conv} is the heat flux density by convection, α is the convection surface heat transfer co-efficient, T_s is the surface temperature and T_a is the ambient temperature. The convection surface heat transfer co-efficient is a function of the thermal properties of the workpiece and the surrounding fluids (gas or air). This mode of heat transfer becomes important when designing low-temperature induction systems (500 deg.C or less) as the convective losses in these applications are equal to or exceed the heat losses due to radiation [9].

4.D.1.3. Thermal Radiation

Thermal Radiation may occur due to heat transfer from the workpiece to the surrounding that include a non-material region (vacuum). The phenomenon of thermal radiation is often described as the propagation of electromagnetic energy due to a temperature difference. It is governed by the Stefan-Boltzmann law which states that the heat transfer rate by radiation is proportional to a radiation loss co-efficient C_s and the value of $T_s^4 - T_a^4$. As can be seen, since the radiation losses are directly proportional to the fourth power of temperature, these losses form a significant part of the total losses in high-temperature applications [9].

4.E. Magnetic Flux Control Techniques

Flux is defined as the rate of transfer of fluid, particles or energy across a given surface interface. Magnetic flux is a measure of the total number of magnetic field lines crossing a chosen surface. Even if magnetic flux lines cannot be seen, they can be represented in the form of mathematical calculations and graphs. Since an isolated magnetic source has never been observed to exist, the net flux of the magnetic flux density vector (B) is always zero. Therefore, the lines of a magnetic field are closed loops and for a given volume, the number of lines entering the volume will always be equal to the number of lines leaving the volume. There are several ways through which the position of these lines can be altered. The density can be changed by changing the cross-section through which these lines pass or through which the flux flows. The positions of these lines can also be changed by making use of some special materials that give a different path for the flux to flow or restrict the path of

the magnetic flux. The third way is to introduce another current-carrying conductor in the vicinity and then due to the proximity effect, the magnetic flux lines are altered [9].

4.E.1. Electromagnetic Shunts

Magnetic fields in induction heating are generated with the purpose to heat a metal workpiece. However, the field often ends up heating not only the workpiece but also the metal surrounding the coil and workpiece. In order to avoid this, it becomes necessary to make use of magnetic shields to reduce the effect of magnetic field and to protect other structures, components or equipment coupling to the coil [9].

4.E.2. Magnetic Shunts

Magnetic shunts usually consist of large stack of thin steel laminations placed along the axis of the inductor. These provide a parallel and low reluctance path for the magnetic flux. Shunts reduce the external magnetic field and prevent heating of the surrounding metal components when used along with heating coils. They can also be a good source of significant power dissipation in the system and can be cooled by water [9].

4.E.3. Magnetic Flux Concentrators

The main intent of the flux concentrators in induction is to improve the magnetic coupling efficiency and to achieve effective selective heating in workpiece areas that are either complex in geometry or difficult to heat. In the absence of a flux concentrator, the magnetic flux may spread around the coil or current-carrying conductor and may couple with it. The concentrator forms a magnetic channel for the magnetic flux of the coil in a desired area outside the coil. This happens mainly due to the conductor's current getting concentrated

on the surface facing the workpiece. This current concentration leads to good coil-workpiece coupling and therefore improves the coil efficiency by reducing any losses that might occur otherwise. The actual current distribution heavily depends on frequency, magnetic field intensity, geometry and material properties of the conductor, workpiece and also the concentrator. Flux concentrators help in improving the efficiency of the process partly by reducing the coupling distance between the conductive part of the coil and the workpiece. They also reduce the stray losses by reducing the reluctance of the air path. However, the conduction of high-density magnetic flux in the concentrators also generates heat inside the concentrator due to the Joule effect. This leads to a drop in the electrical efficiency. The overall change in the efficiency is a result of the above mentioned three factors. As a result of this, appropriate use of the magnetic flux concentrator becomes necessary to achieve a higher process efficiency. This also results from the concentrator's potential to concentrate magnetic field in a certain area due to which the field does not propagate behind the concentrator. The collective effect of which, the heated mass or area of the metal is smaller and the desired heating pattern is achieved [9].

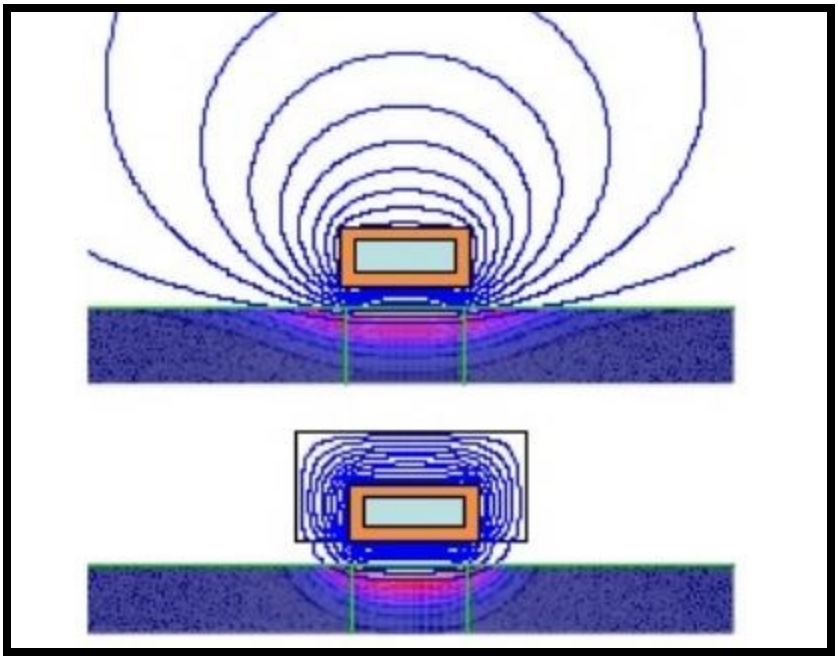

Figure 4.4: Magnetic field without concentrator and with concentrator [25]

4.E.3.1. Selection of Flux Concentrator Materials

Selection of a material for the flux concentrator is influenced by many factors including electrical resistivity, thermal conductivity, relative magnetic permeability, curie point, saturation flux density and ductility. Additional factors include machinability, formability, resistance to any chemical reactions, ability to withstand high temperatures, etc. The materials under consideration should have a high slope of magnetic permeability and a high saturation flux density. Magnetic materials with high electrical resistivities reduce eddy current losses of the concentrator thereby reducing its temperature increase. Having a higher thermal conductivity helps in overcoming local over-heating that is caused, at times, due to radiation from the heated workpiece or high-density flux in some areas of the concentrator. The most commonly used type of materials as flux concentrators are as follows:

1. Laminations
2. Electrolytic iron-based materials
3. Carbonyl iron-based materials
4. Pure ferrites and ferrite-based materials
5. Soft formable materials

The use of soft formable materials helps in ease of molding of flux concentrators as per desired shape and size and later machining, if needed, to exact tolerances. One such material is Alphaform which is an advanced composite made of insulated-iron microparticles, space-age polymers and a thermally sensitive catalyst.

Some of the advantages of using flux concentrators are listed as follows:

1. Reduce the operating power levels required to obtain the desired heating of the workpiece.
2. Improve the electrical efficiency of the process and decrease the amount of energy used.
3. Make selectively heating of specific areas of the workpiece possible.
4. Obtain a superior heat pattern and improve the physical and metallurgical properties.
5. Minimize geometric distortion of the workpiece.
6. Prevent undesirable heating of the adjacent parts or areas of the workpiece.
7. Improve equipment life.
8. Reduce cycle time [9].

4.F. Application of Induction to Control Thermal Distribution in AM

As discussed in Chapter 3, controlling the thermal distribution in the powder bed becomes extremely crucial in terms of porosity control, formation of residual stresses, crack initiation, curling, balling and the overall build quality of the parts. Also, significant enhancements in the material properties of the powder metal can be achieved by maintaining constant thermal cycles and temperature profiles throughout the process. Techniques have been developed in order to address the thermal distribution and the issues that follow with it. Research has been made where induction coils are introduced along the edges of the powder bed to control the variation of temperature at different depths of the powder bed in order to achieve a gradual thermal gradient during the process [20]. However, not much has been contributed towards minimizing power consumption and optimizing thermal distribution at the same time by minimal modification in the conventional powder bed setup.

Induction to heat the powder instead of heating the entire bed is proposed through this study after taking into consideration the benefits of Induction heating that can be suitably applied to the Additive Manufacturing process. The introduction of induction or induction coils to selectively heat the powder substrate will not only help in minimizing the power usage due to lower requirements of laser power, no arrangement required to maintain the powder-bed temperature but also as a result of this, will increase the process efficiency. The proposed technique will also help in improving cost benefits in terms of powder re-usability. In a typical SLS setup, as the powder bed is heated, the powder that acts as a

support structure to the part being built cannot be re-used directly. This is because the powder undergoes thermal variation throughout the build-time of the process reducing its material properties. Due to this, post-processing of the unused powder becomes necessary if the same powder needs to be re-used. This also calls for time-delays in production. A new process has recently been introduced to address this issue. It is known as Micro-Induction Sintering. However, the process makes use of induction operating at Radio-Frequency as the only source of heat generation for sintering of powders [21]. The implementation of induction coils operating at a medium frequency range (280-340 kHz), thus becomes more practical. The unique advantages of induction such as the skin effect, reference depths thus become operational parameters and, therefore, they can be tuned to optimize the process as per the requirement. Also, the quick response time of metals while heating through induction helps in reducing the cycle time of the process.

One of the most important factor of this proposition lies in achieving a certain temperature within a minimal heat affected zone (HAZ) in shortest time possible. In order to achieve this, flux concentrators are used to not only increase the flux density but to also channel it through the path requirement for a given geometry. Based on the above discussion, simulations are carried out for a simple Cylindrical Coil to benchmark parameters and also to validate the concept. Further modifications are then made purely based on optimization of coil design and heating requirements. Alphaform MF from Fluxtrol Inc. is used as the flux concentrator due to its material properties aligning with the process requirements. The following table gives an overview of the properties of Alphaform MF:

Properties	Units	Alphaform MF
Density	g/cm3	4
Maximum Permeability	none	10
Saturation Flux Density	T	0.9
Operating Frequency Range	kHz	10-1000
Thermal Conductivity	W/(cm.deg.C)	0.02

Table 4.1: Properties of Alphaform MF [25]

Actual heating trials are then carried out based on the design and process parameters obtained through simulations. A detailed discussion about this design of experiments is mentioned in the following chapter.

Chapter 5 Experiments and Simulations

Based on the literature and concept generation in the previous chapters, the next step in this study was to run simulations of induction with a process specific induction coil, determination of process parameters for induction and also study its effects on different substrates. The first step in this stage was to start simulations for a simple cylindrical coil. Out of the different materials used commercially, Stainless Steel 410 was chosen as the primary substrate due to its martensitic properties. The coil design had to be small and lightweight in order to be able to accommodate the coil in any complex working environment. As a result of this, it was decided to fabricate a coil out of a 1/8" OD Copper tubing. COMSOL Multiphysics 5.3a was used to simulate the induction process with the Heat Transfer in Solids and the AC/DC modules.

Based on the discussion of skin effect in Chapter 4, calculations were carried out for the SS powder to obtain the value of the reference depth. From the equation, for a variation of frequency from 280 kHz to 320 kHz, the reference depth value varies from 3mm to 3.2mm. As a result of this, a 3mm thick substrate was modelled under the coil with an air-gap of 2mm between the two. A cylinder of the height of 0.5in was modelled as the cylindrical coil having four turns of the 1/8" copper tubing assuming the turns of the coil are closely wound to each other to avoid any losses due to proximity effect. Simulations were carried

out at 40A to check for temperature rise. All simulations for the cylindrical coil were carried out at 320 kHz and the ambient (initial) temperature was considered to be 25deg.C

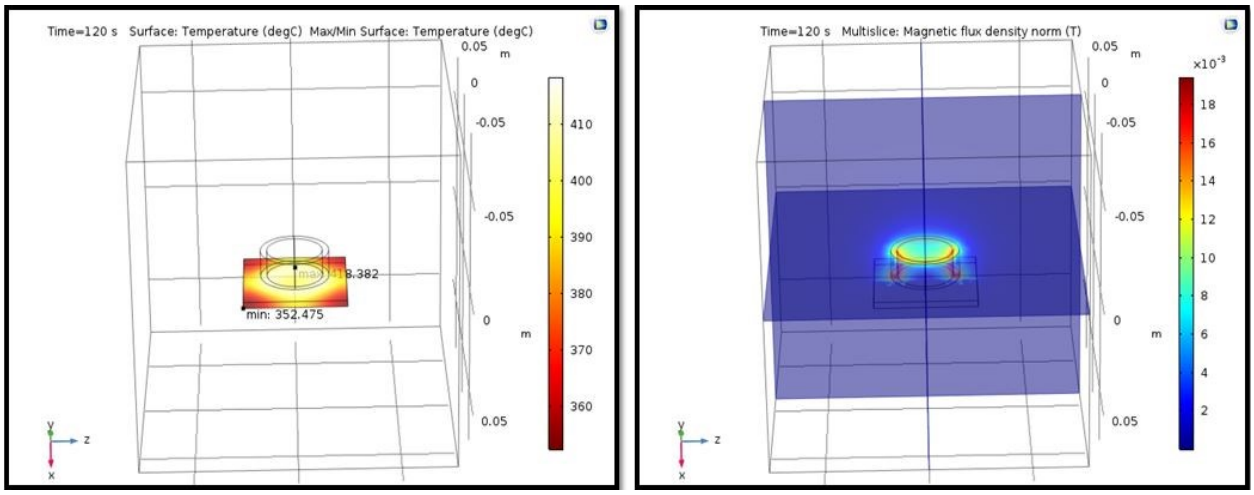

Figure 5.1: Surface temperature and Magnetic flux density for a 4 turn Cylindrical Coil

As can be seen from Figure 5.1, the maximum temperature obtained for a heating trial of 2mins was ~419 deg.C and the magnetic flux density was $18*10^{-3}$T. The next step was to improve the efficiency of the coil by making changes to the design of the coil to obtain higher temperatures and also better coupling through higher magnetic flux density.

One more observation through the pilot simulation was the HAZ. It was found that the area of the HAZ was directly related to the surface area of the coil facing the substrate. However, a minimal HAZ would be required to validate the concept as per the proposal. Due to these conclusions, suitable changes then had to be made to the design of the coil and further literature survey was done to study the magnetic field for a given geometry. The spherical conical induction coil was found matching closely to all the requirements of the proposal. The distribution of the magnetic field in such a conical coil was also studied and it was studied to be as follows:

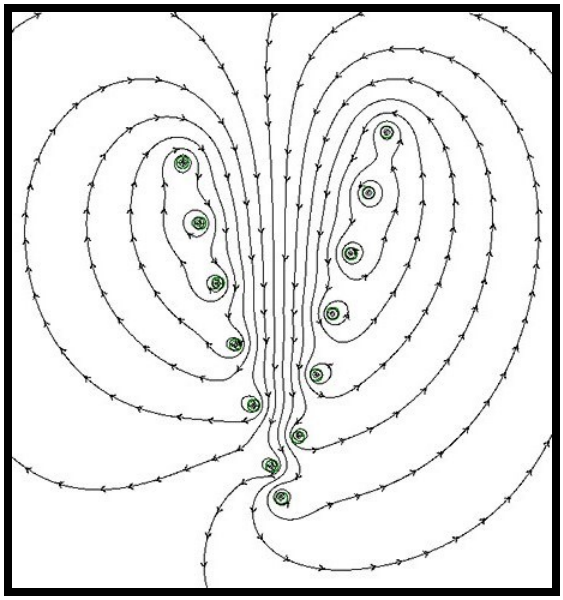

Figure 5.2: Representation of magnetic field of a single cone coil [24]

The intensity of the magnetic field density on the inner side of the cone could then be put to maximum use in the case of this study. Once the shape of the coil was decided, the cone angle, the coil height and the diameter of the top surface had to be finalized. To start with, the cylindrical coil model was then modified to a conical coil with the angle of the cone to be 18 degrees. The diameter and the height of the cylindrical coil was kept constant for the conical coil. The air gap between the coil and the substrate was also increased to 3mm. This coil was crudely turned on a cone 3D printed with the help Stratasys 400mc. 3 inch SS 41C powder compacts were made with the use of a molding press. This was done as a means of replicating the compacted powder in the powder bed. The coil was then checked for coupling effeiciency on the basis of temperature rise with the help of Pillar MK-20 Induction system.

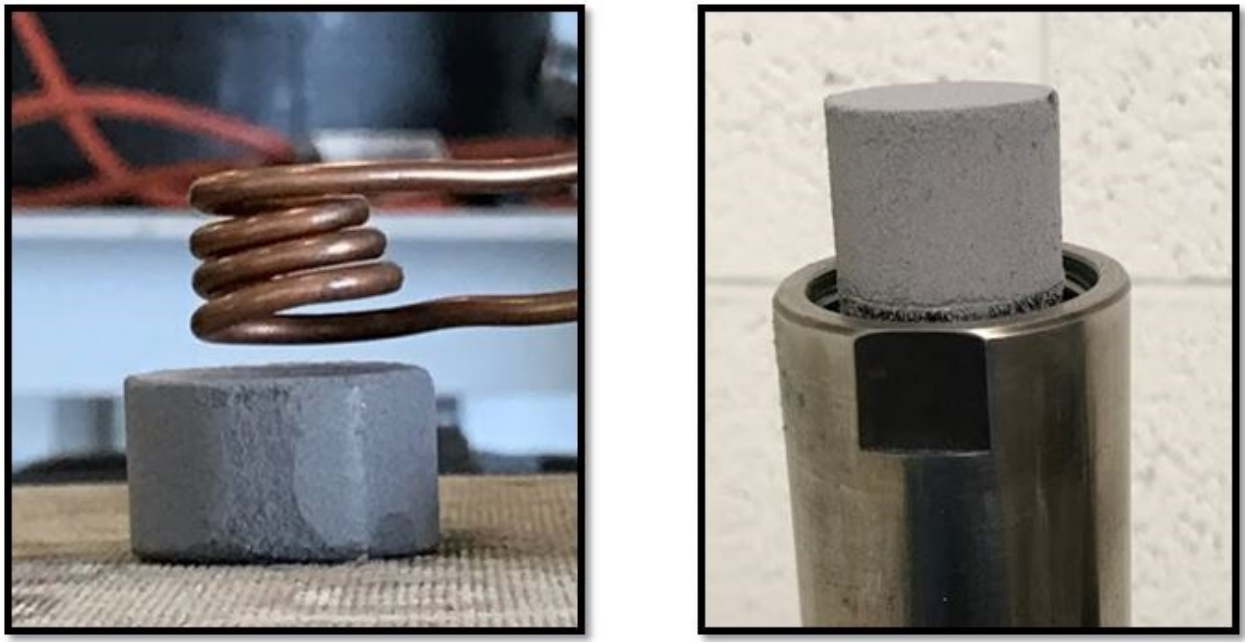

Figure 5.3: SS 41C powder compact tested out with a 4 turn induction coil (left) and the SS 41C powder compact being made on the molding press (right)

This system automatically adjusts the frequency according to the load attached to the machine. The machine has a water recirculation system that helps in conducting the current to the coil and also in cooling the coil during the process. The heating trial did not yield satisfactory outcome as a temperature rise of only 110deg.C was observed at the end of the 2 minute heating trial. Conclusions were made that the coil design had to be optimized to improve the coupling efficiency. Also, the relatively small rise in temperature indicated that an alternative mechanism to couple the coil with the powder had to be studied.

As a part of this study, the orientation of the coil was changed and the coil was now flipped upside down. Simulations for the same coil were then carried out for te 3mm thick SS410 substrate. However, as can be seen from Figure 5.4, the increase in the magnetic flux and decrease in the HAZ compromised the rise in temperature. A temperature rise of 236 deg.C was obtained in a span of 2 mins. The magnetic flux density increased to $4*10^{-3}$T. This

lead to the next step of the simulation where a more acute angle of symmetry was simulated. The angle of the cone was now changed to 16 degrees and rest all of the parameters were kept same.

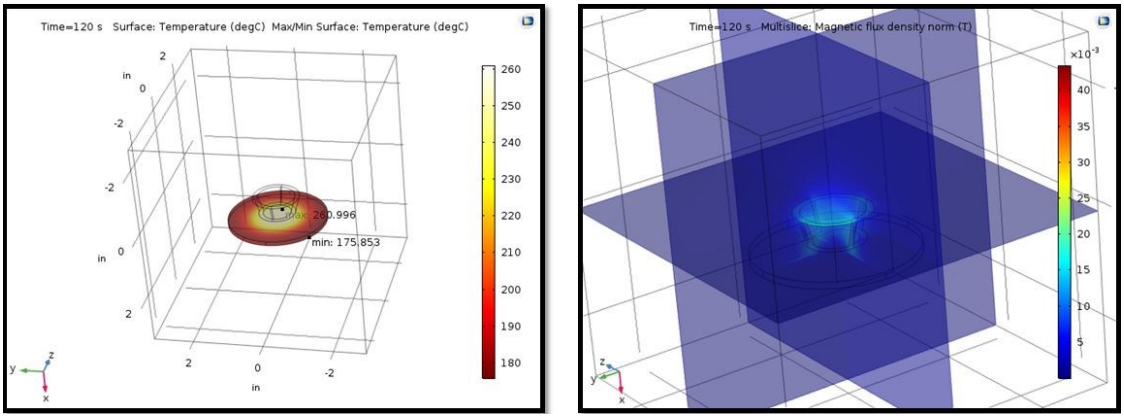

Figure 5.4: Surface temperature and magnetic flux density for a 4 turn conical coil with a 18 degree cone angle

The 16 degree cone angle coil simulated improved temperature rise with a slight decrease in the magnetic flux density (25*10^{-3} T). The HAZ zone however also showed some change through visual inspection. A change of 2 degrees on the angle of the cone showed a drastic rise in temperature from 236 deg.C to 390 deg.C for the same set of parameters. The results of the simulations are as shown in Figure 5.5.

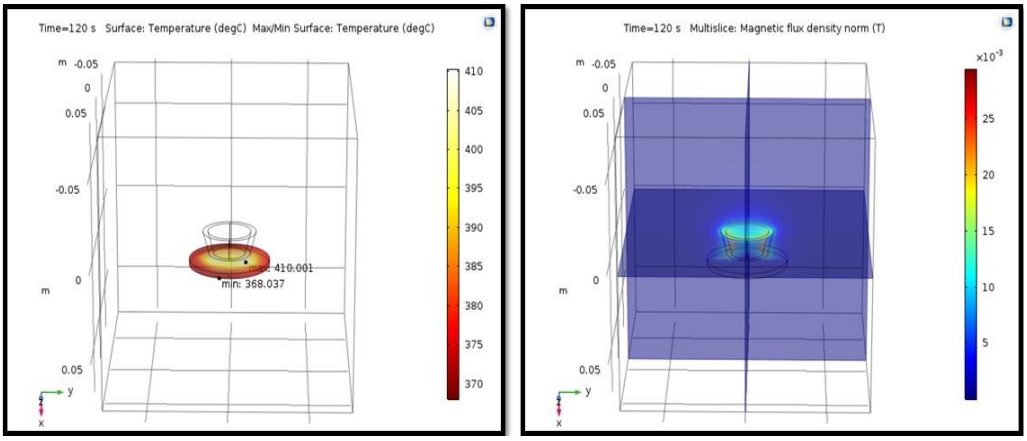

Figure 5.5: Surface temperature & magnetic flux density for a 4 turn conical coil with 16 deg. cone angle

To maintain a constant thermalcycle and a temperature closer to $0.5T_{melt}$ of the metal, it then became necessary to make use of flux concentrators. The unique advantages of flux concentrators as discussed in the previous chapter would help increase the magnetic flux density and also in reducing the HAZ leading to an increase in temperature rise. Alphaform MF from Fluxtrol was used as a flux concentrator due to its formability and properties suiting the range of frequency of operation. An approximate layer of 4mm of Aphaform MF was applied on the inner side of the 4 turn conical coil.

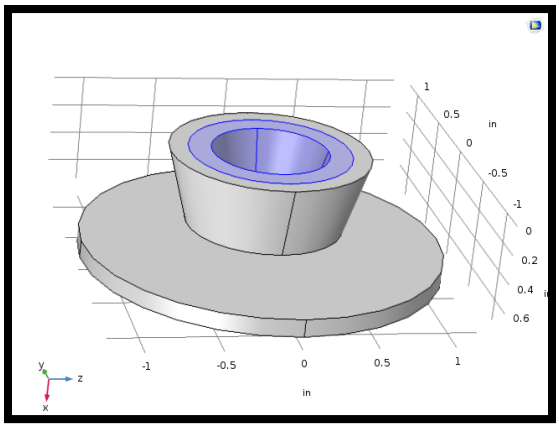

Figure 5.6: Application of fluxtrol to the 4 turn conical coil (highlighted in blue)

The rest of the parameters were kept constant from the previous simulation. The simulation results showed a significant rise in temperature from 390 deg.C to 582deg.C. Also a reduced HAZ was observed due to the addition of a flux concentrator with the magnetic flux density increasing from $25*10^{-3}$ T to 0.06T. The results are as shown in Figure 5.7.

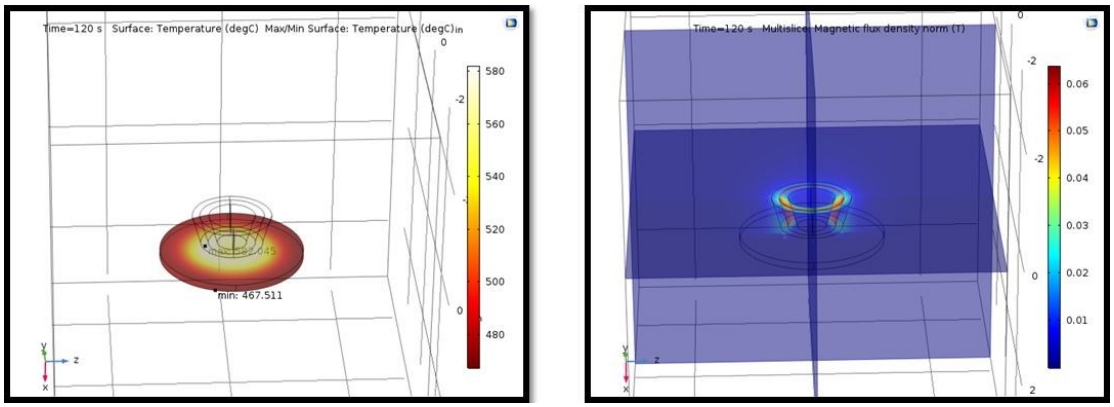

Figure 5.7: Surface temperature & magnetic flux density for a 4 turn conical coil with a 16 degree cone angle and Alphaform MF

To validate the results obtained from the simulations of the induction coils, a physical coil was fabricated with the help of fixtures 3D printed from the Fortus 400MC at the Additive Manufacturing Processes Lab at the University of Michigan-Dearborn. The 1/8" copper tubing was wound around these fixtures and then turned out to separate them from the fixture. An illustration of these fixtures is as shown in Figure 5.8.

Figure 5.8: Copper tubing wound around a 3D printed fixture

Alphaform MF was then added on to the coil thus obtained. Stepwise instructions to add the flux concentrator to the coil were followed as provided by the manufacturer. The Pillar MK-20 Induction system was then used to carry out the actual heating trial for the coil. A frequency of 320 kHz was obtained due to the load thus attached.

Figure 5.9: Images of heating trials with a 4 turn conical coil with Alphaform MF applied on the inner side of the coil

Temperature measurement was carried out with the help of Infrared Thermometers. The thermometers did not read accurate temperatures due to the heavy reflections coming from the substrate while heating up. As a result, the temperature reading was always taken at the beginning of the trial and at the end of the trial to minimize the error in the measurements. It was observed that the temperatures obtained through the actual heating trial were close to the readings obtained through the simulations. As can be seen from Figure 5.9, the HAZ was only spread as big as the surface of the coil facing the substrate. The ambient (initial) temperature was measured to be 28.5 deg.C and the final temperature was noted at 625 deg.C i.e., a total temperature rise of ~595 deg.C was obtained. This result was very close to the measurement obtained through COMSOL (582 deg.C).

The next step involved spreading the SS 41C powder onto the substrate and couple the same coil to the substrate beneath the powder so as to heat the powder through all the three modes of heat transfer.

This step included conducting heating trials in two stages. The first stage included heating an approximate 1 mm thick powder layer on a SS substrate. The frequency of operation of both the stages was 320 kHz. The maximum input current given was 40A.

Figure 5.10: Substrate with SS 41C powder after heating trial

A temperature rise of 500 deg.C was achieved in the first stage of the heating trial. In the second stage of the heating trial, a new substrate was used and the first stage was repeated. After a time delay of 1 min, a second layer of powder was spread onto the heated powder and substrate. However, a steady temperature rise of ~500 deg.C was obtained for both the trials in the second stage. This served as an indication that a steady temperature profile could be obtained for a powder layer as thick as 2mm. The heated substrate is as shown in Fig 5.11

Figure 5.11: Heated substrate with 2 layers of SS 41C powder 1mm each

To now obtain a temperature rise close to $0.5T_{melt}$, further modifications were made to the coil design. The coil height was now increased by adding two more turns to the 4 turn coil. The angle of the cone was kept constant at 16 degrees and the also rest of the parameters unchanged.

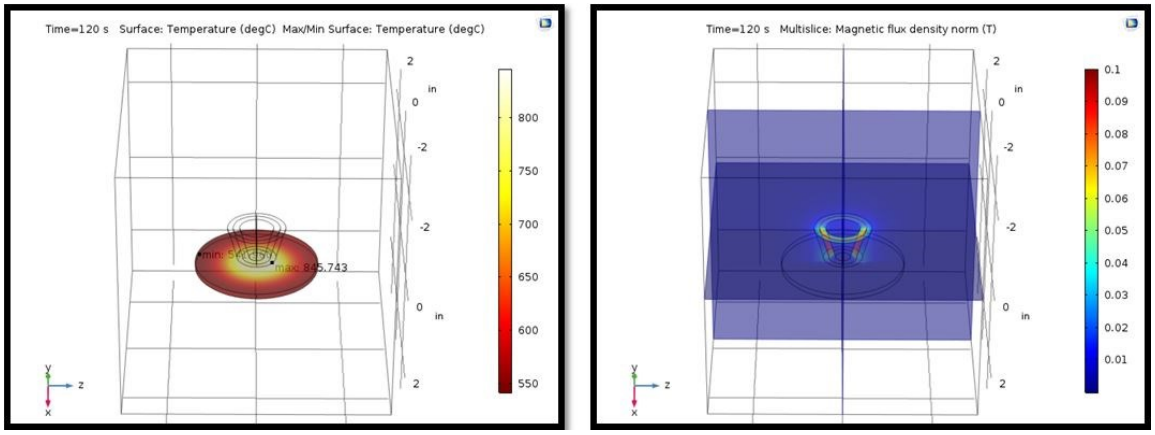

Figure 5.12: Surface temperature & magnetic flux density for a 6 turn conical coil with a 16 degree cone angle and Alphaform MF

The results showed a temperature increase of 820 deg.C with a smaller HAZ and an improved Magnetic Flux Density of 0.1 T. On comparison of the entire flow of simulations, the optimization of the design parameters of the coil had led to a significant increase in temperature difference (~410 deg.C) and a significant increase in the magnetic flux density ($18*10^{-3}$ T to 0.1 T). The spread of the magnetic field with and without the use of flux concentrator was also compared through the simulation results of the 6 turn conical coil. It was clear through simple observation that the flux concentrator helped in channeling the flux. This was also supported by the increase in the magnetic flux density from 0.05T to 0.1T by the addition of Alphaform MF.

The last step in the stage of simulations was to simulate the same coil design for different substrates. For this, SS316L, SS304 and Titanium were chosen. Simultaneously, simulations for each of the above mentioned substrates were carried out. Due to the austenitic properties of the substrates, the process demanded a higher current input. As a result of this, for a current input of 50A, a temperature of 812 deg.C was obtained for SS316L, 810 deg.C for SS 304 and 723 deg.C at 80A for Ti.

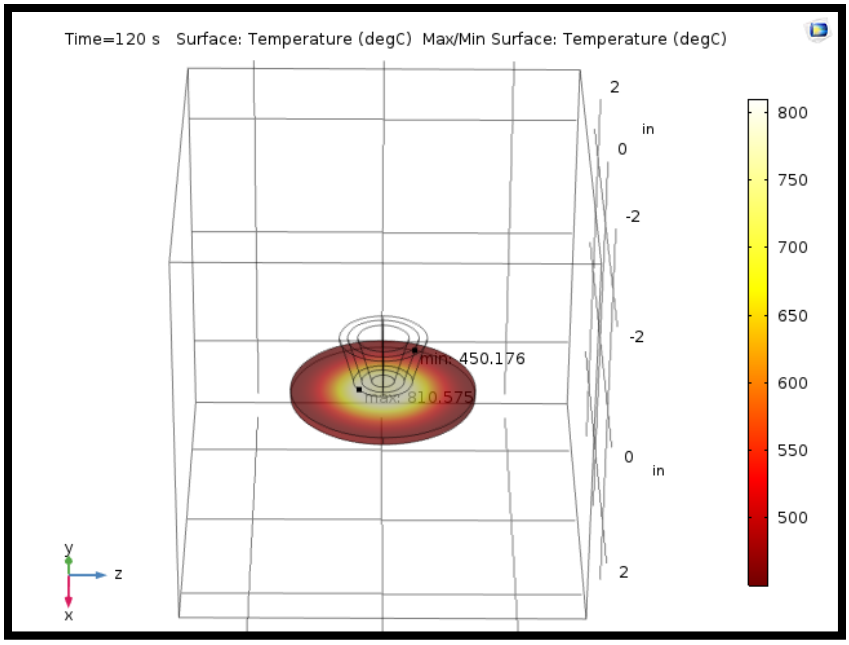

Figure 5.13: Surface temperature of SS304 for a 6 turn conical coil with Alphaform MF

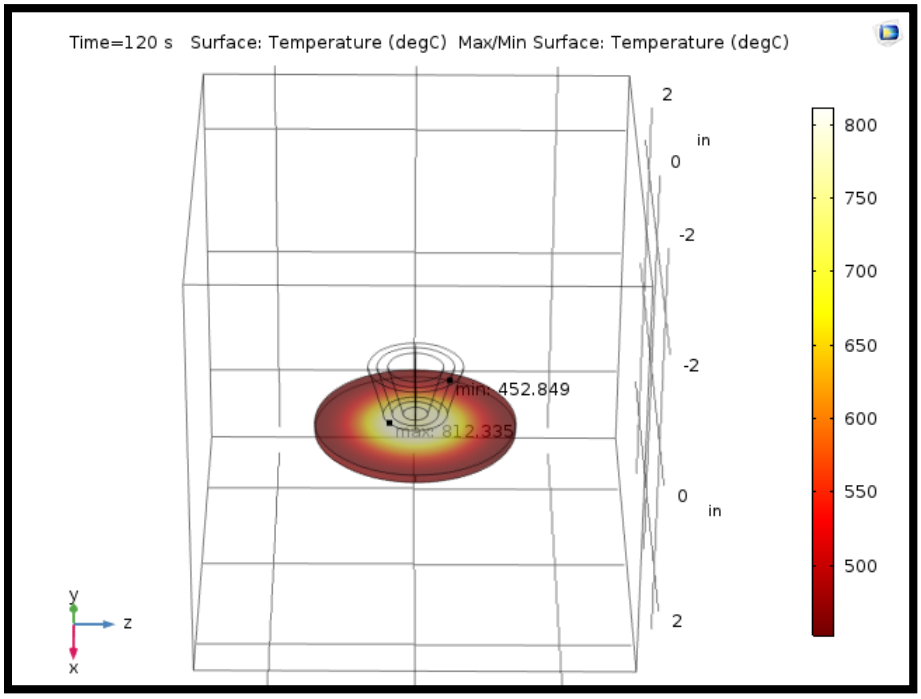

Figure 5.14: Surface temperature of SS316L for a 6 turn conical coil with Alphaform MF

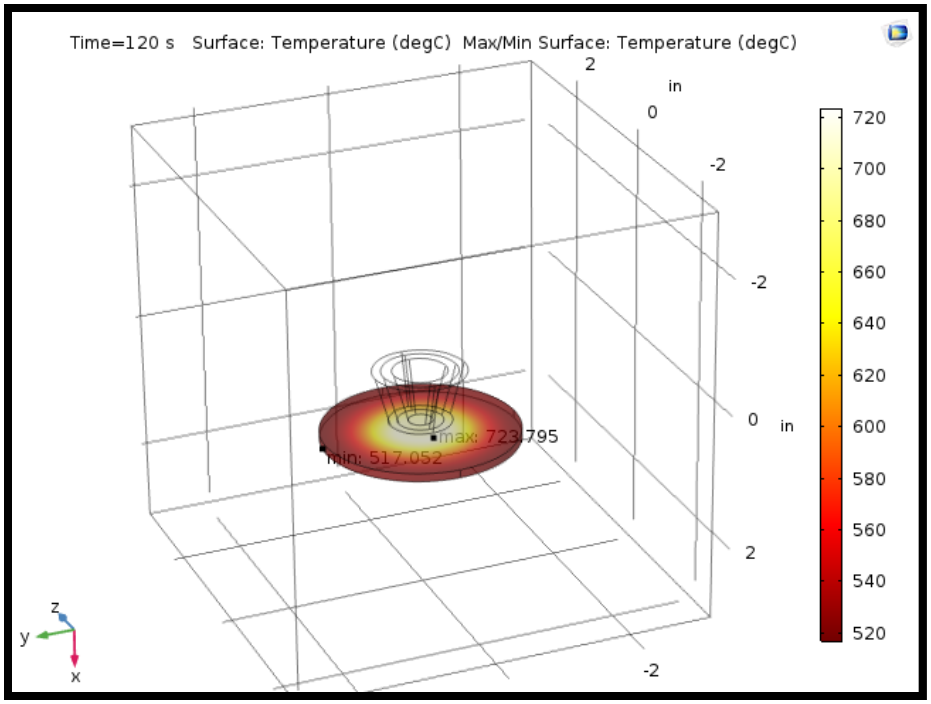

Figure 5.15: Surface temperature of Titanium for a 6 turn conical coil with Alphaform MF

Therefore, in conclusion, it was observed that the optimization of coil design had helped to improve the magnetic flux density and obtain the required temperature rise. One of the most influencing factor in the simulations of the induction coil was the use of flux concentrator i.e., Alphaform MF. A constant thermal profile was obtained through actual heating trials carried out on SS 41C powder layers. The following table lists out the specific comparisons of the different types of induction coils modelled for the simulations and the corresponding changes in the magnetic flux densities and temperature readings achieved for the SS410 substrate.

Coil	Magnetic Flux Density (T)	Temperature (deg.C)	Current (A)	Frequency (kHz)
Cylindrical Coil	18 x 10-3	419	40	320
4 Turn Coil (18 degree)	4 x 10-3	236	40	320
4 Turn Coil (16 degree)	25 x 10-3	390	40	320
4 turn MFC Coil	0.06	560	40	320
6 turn MFC Coil	0.1	820	40	320

Table 5.1: Overall results of COMSOL Simulations for the induction coils

The “4 turn MFC Coil” and the “6 turn MFC Coil” are the coils that were modelled with the Magnetic Flux Concentrator (Alphaform MF) on the inner side of the coil.

Chapter 6 Scope and Conclusion

The proposed method of auxiliary heating the substrate so as to control the thermal distribution and selectively heat as per the requirement provided satisfactory results through simulations and actual heating trials. The use of flux concentrators on the coils helped concentrate and channelize the magnetic flux along the desired path and heat the substrate better and faster. Different grades of steel and titanium were successfully simulated and tested out. This ensured minimal changes in operational parameters to easily adapt to substrates with different material properties. The proposed design of the induction coil is small enough to be a convenient addition to any complex environment for improved heating.

However, there still lies a window for improvement and a much broader scope for the proposed concept. Metals such as Stainless Steels, Titanium, Copper, and Aluminum find great applications in the Additive Manufacturing Industry. Specially, metals like Aluminum and Copper have high thermal conductivities and act as heat sinks. This makes it difficult to heat and sinter these metals. The proposed concept can further be studied and improved to work with metals like Aluminum and Copper so as to broaden the application scope of the proposed technique in the industry.

Also, the simulations and the experimental data presented in this study limits itself to stationary heating of the substrate. Work still is in progress to study the effects of induction in translational motion and the required changes that will follow. These changes may be in terms of coil design modification or process optimization by fine tuning the parameters. The phenomenon of induction heavily relies on the coupling efficiency of the coil and the substrate. This study provides good highlight over the improved magnetic flux density and a more contained magnetic field for substrate having a horizontal orientation. A detailed study of the effect of different orientations (e.g.: vertically orienting the substrate) on the coupling efficiency and thermal distribution would play an important role in applying the proposed technique to any Additive Manufacturing process.

The Pillar MK-20 system used for the heating trials of the induction coil automatically adjusts the frequency of operation as per the load. However, this frequency is set through a pre-determined minimum range of frequency. This range can be adjusted by changing the capacitance of the system and then lowering or increasing the frequency range as per the requirement. This would allow to optimize the entire process of induction.

To make the proposed concept more robust, new coil designs can be modelled and simulated to improve overall efficiency of the system and with relatively lower power requirements.

Bibliography

1. Additive or Subtractive Prototyping: Which is best?- Protomatic 09/05/2017 9:42am
2. Standard Terminology for Additive Manufacturing Technologies- ASTM 09/05/2017 10:00am
3. https://www.forbes.com/sites/tjmccue/2016/04/25/wohlers-report-2016-3d-printer-industry-surpassed-5-1-billion/#52cd00b119a0 09/05/2017 11:08am
4. http://www.robots-and-androids.com/history-of-3d-printing.html 09/05/2017 3:16pm
5. http://www.additivemanufacturing.media/cdn/cms/7_families_print_version.pdf 09/06/2017 8:45am
6. Consolidation of Polymer Powders by Selective Laser Sintering J.-P. Kruth1 , G. Levy2 , R. Schindel2 , T. Craeghs1 , E. Yasa1 1K.U. Leuven, Division PMA, Heverlee, Belgium 2 Inspire AG, IRPD Institute for Rapid Product Development, St. Gallen, Switzerland 09/06/2017 8:58 am
7. https://www.thoughtco.com/electromagnetic-induction-2699202 09/06/2017 11:40 am
8. http://induction.fivesgroup.com/our-expertise/induction-heating/the-concept-of-induction-heating.html 09/06/2017 4:27 pm
9. Handbook of Induction Heating: Valery Rudnev, Don Loveless, Raymond Cook, Micah Black 04/16/2018 4:55pm
10. History of Additive Manufacturing, Wohler's Report 2014: Terry Wohlers and Tim Gornet 07/02/2018 11:26pm
11. https://designandmotion.net/design-2/manufacturing-design/dmls-a-little-history/ 07/03/2018 10:02am
12. https://www.allthat3d.com/3d-printing-history/ 07/03/2018 10:28pm
13. 3-D printing: The new industrial revolution: Barry Berman 07/0382018 2:50pm
14. Selective laser sintering: A qualitative and objective approach: Sanjay Kumar 07/09/2018 9:50am
15. Balling Process in Selective Laser Sintering 316 Stainless Steel Powder: Y.F. Shen1,a, D.D. Gu1 and Y.F. Pan, 1College of Materials Science and Technology, Nanjing University of Aeronautics & Astronautics, Nanjing, 210016, China 07/09/2018 10:00am
16. Consolidation phenomena in laser and powder-bed based layered manufacturing: J.-P. Kruth1 (1), G. Levy2 (1), F. Klocke3 (1), T.H.C. Childs 4 (1)- (1) K.U.Leuven, Division PMA, Leuven, Belgium, (2) FHS - University of Applied Sciences St.

Gallen, Switzerland, (3) Fraunhofer, Institute for Production Technology IPT, Aachen, Germany, (4) University of Leeds, School of Mechanical Engineering, UK 07/11/2018 10:12am

17. Temperature Gradient Mechanism: Overview of the Multiple Pass Controlling Factors: S. P. Edwardson, J. Griffiths, G. Dearden, K. G. Watkins, Laser Group, Department of Engineering, University of Liverpool, L69 3GQ, UK 07/12/2018 2:23pm
18. Review of selective laser melting: Materials and applications: Chor Yen Yap, Swee Leong Sing, L.E.Loh 07/12/2018 4:52pm
19. A study on shrinkage compensation of the SLS process by using the Taguchi method: H.-J. Yang a, P.-J. Hwang a, S.-H. Lee 07/12/2018 5:14pm
20. Sintering and Laser Fusion Device, comprising a means for heating powder by induction: Theirry Flesch, Jean Baptiste-Mottin, USA Patent No: US 9,616,458 B2 07/17/2018 10:52am
21. Additive Manufacturing/Diagnostics via the High Frequency Induction Heating of Metal Powders: The Determination of the Power Transfer Factor for Fine Metallic Spheres: Grid Logic Inc., 07/17/2018 12:39pm
22. A Review on Powder Bed Fusion Technology of Metal Additive Manufacturing Valmik Bhavar, Prakash Kattire, Vinaykumar Patil , Shreyans Khot , Kiran Gujar , Rajkumar Singh Kalyani Centre for Technology and Innovation (KCTI), Bharat Forge Ltd., Pune, India 09/06/2017 11:15 am
23. Specification and Use of a Flux Concentrator: Mr.Robert Ruffini 07/17/2018 9:41am
24. Magnetic field of Conical Coil: Simulating the STA Magnetic Field: Bashar Space-Time Antenna 07/18/2018 10:25am
25. https://fluxtrol.com/alphaform-MF 07/19/2018 3:28pm
26. Microstructural characterization of Thin and Thick directional Ti-6Al-4V structures using Laser Deposition Process: Ramcharan Palacode Visveswaran